Experimental studies on the defect states at the interface between nanocrystalline CdSe and amorphous SiO_x

2000 J. Phys.: Condens. Matter 12 751

(http://iopscience.iop.org/0953-8984/12/5/320)

J. Phys.: Condens. Matter **12** (2000) 751–759. Printed in the UK PII: S0953-8984(00)05981-6

Experimental studies on the defect states at the interface between nanocrystalline CdSe and amorphous SiO_x

D Nesheva†§, Z Levi†, Z Aneva†, V Nikolova† and H Hofmeister‡

† Institute of Solid State Physics, 1784 Sofia, Bulgaria
‡ Max Plank Institute of Microstructure Physics, D-06120, Halle, Germany

E-mail: nesheva@issp.bas.bg

Received 13 July 1999

Abstract. Superlattices of a-SiO_x/nc-CdSe and thin composite films of SiO_x doped with CdSe nanocrystals have been investigated. The CdSe nanocrystals size in both kinds of samples was determined by x-ray diffraction and HREM measurements. A significant difference has been found in the size values determined by both methods, which has been ascribed to appreciable nanocrystal lattice deformations. Subband absorption, room-temperature photoluminescence and thermally stimulated currents have been measured. It has been observed that in the superlattices the absorption in the tail region increases as sublayer thickness decreases. A new photoluminescence band has also appeared in the superlattices having thinnest (2.5 nm) CdSe sublayers. Two new maximums at about 220 K and 240 K, not existing in the CdSe single layers studied, have been found in thermally stimulated current spectra of the composite films. Both maximums are less expressed in the superlattices. The described results have been connected with a size-induced increase in the concentration of interface defect states in CdSe nanocrystals. It has been estimated that these defects are disposed at about 0.35 eV above the highest occupied molecular orbit in CdSe.

1. Introduction

Glasses doped with semiconductor microcrystals are promising as novel nonlinear optical materials. Special attention has been paid to glasses doped with CdS_xSe_{1-x} microcrystals which are available as commercial colour glass filters. In these filters the maximum values of $\chi^{(3)}$ reported are 10^{-7} esu and the shortest relaxation times are $\sim$10 ps [1, 2]. The quantum confinement effect, the presence of trap levels within the gap and the surface itself strongly affect many properties of these materials [3–5]. From the measured magnitude of the nonlinearity, it is concluded that, most probably, carriers trapped in surface defect states act through the static electric field they created [5]. On the other hand, the recombination through defect states in the gap of Cd-chalcogenide microcrystals has a strong influence on their photoluminescence spectra [6, 7]. However, as the properties of semiconductor doped glasses are rather complex, the information concerning the energy position of levels associated with the defect states is still rather scanty.

In this article CdSe nanocrystals (NCs) embedded in SiO_x thin-film matrix as well as SiO_x/CdSe superlattices (SLs) of nanocrystalline CdSe layers alternated by amorphous SiO_x layers have been studied. The specific way of producing CdSe NCs in SiO_x matrix employed [8] enabled us to measure and compare photocurrent spectral dependences and

§ Correspondence author.

0953-8984/00/050751+09$30.00

thermally stimulated currents (TSC) in both groups of samples. The results from the electrical measurements have been considered in combination with those obtained from room-temperature photoluminescence studies, thus the energy position of some interface-induced defects in CdSe NCs embedded in SiO_x has been estimated.

2. Experimental details

Two groups of samples: (I) SiO_x/CdSe multilayers and (II) CdSe NCs embedded in SiO_x ($x \approx 1.5$ [8]) thin-film matrix were prepared by thermal evaporation of CdSe and SiO from two independent alternatively heated tantalum crucibles in vacuum of 10^{-3} Pa. Substrates of Corning 7059 glass were used, maintained at room temperature during the deposition procedure. The sublayers of CdSe in both groups of samples as well as SiO_x sublayers in the multilayers were deposited in a step-by-step way and their thickness was controlled during deposition by means of a quartz thickness and deposition rate monitor MIKI-FFV. More details concerning the procedures of producing samples of each kind have already been described elsewhere [8–10]. The CdSe sublayer thickness in the multilayers here studied was varied between 2.5 and 10 nm as the thickness ratio of SiO_x and CdSe sublayers was kept 1.3. The small-angle x-ray diffraction studies performed on the SiO_x/CdSe multilayers [11] have revealed a good superlattice periodicity. The total thickness of all superlattices here studied was about 0.2 μm. The second group of samples had a total thickness of about 1.5 μm and a constant CdSe doping level of 5 vol%. To improve CdSe NC structure and the mechanical stability of the SiO_x matrix [8], all studied samples were annealed for 90 min in air at 673 K.

In order to determine the average size of CdSe NCs, x-ray diffraction studies were performed on both groups of samples as well as on a slide of Corning 7059 glass (1 mm thick). A Siemens D-500 diffractometer and Cu K_α line ($\lambda = 0.154$ nm) were used. It has been estimated that the x-ray diffraction from the substrate did not affect significantly (figure 1) the shape of the (110) band of wurtzite CdSe. The Scherrer's equation $d = \lambda/\delta 2\Theta \cos\Theta$ was employed to this band in order to calculate the average nanocrystallite diameter d. Here Θ and $\delta 2\Theta$ are the position and full width at half maximum of the band. Besides, the size of CdSe NCs was determined from high-resolution electron microscopy (HREM) measurements performed by means of a JEM 4000 EX operating at 400 kV. Electron micrographs were recorded at 500 000 times magnification using optimum contrast conditions (near Scherzer defocus).

The samples for the electrical measurements were provided with planar contacts (10 mm long and 1 mm spaced) of In–Ga alloy for the SLs and Al or Ag for the samples of the second group. They showed linear current–voltage characteristics at the fields of 10^2–10^3 V cm^{-1} we applied. The constant photocurrent method (CPM) [12–14] was employed in order to study the Urbach tail and band edge absorption of CdSe in the 1.45–2.6 eV energy region. Samples were illuminated by a chopped (2 Hz) monochromatic light from a diffraction grating monochromator MDR 2 at a spectral resolution of 4 nm. Thermally stimulated currents were measured at a rate of 0.05 K s^{-1}. The traps in CdSe NCs were preliminary filled up at 77 K by a 5 min illumination of the samples with white light having a power density of 50 mW cm^{-2}.

3. Results and discussion

3.1. Average nanocrystallite size

X-ray diffraction pattern from a SiO_x/CdSe SL having CdSe sublayer thickness of 5 nm is shown in figure 1. Employing the Scherrer's equation, a value of about 2.5 nm has been obtained for the average size along the $\langle 110 \rangle$ direction of CdSe NCs in this SL. The NC

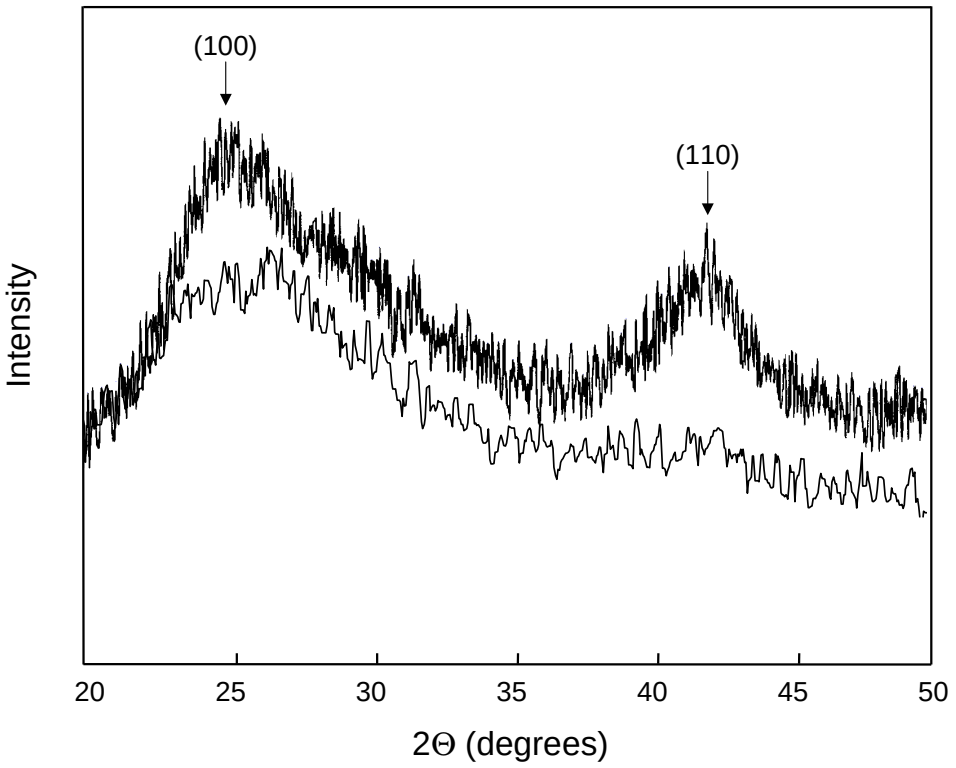

Figure 1. X-ray diffraction patterns of a SiO_x/CdSe superlattice having CdSe sublayer thickness of 5 nm (upper curve) and of a Corning 7059 glass substrate (lower curve). Both spectra were measured at the same collection time and correspond to the same scale. It is seen that x-ray diffraction from the substrate does not appreciably affect the shape of the (110) band. The average diameter of CdSe nanocrystals has been calculated employing Scherrer's equation to the (110) band of wurtzite CdSe.

sizes determined in all SLs studied were approximately twice as small as the thickness of the respective CdSe sublayers. A HREM micrograph of a SiO_x(5.8 nm)/CdSe(4.5 nm)/SiO_x (5.8 nm) structure annealed for 90 min at 673 K is given in figure 2. It is seen from the figure that, the size of CdSe nanocrystallites along the SL axis is equal to the sublayer thickness, i.e. it is twice as great as the average diameter obtained from the x-ray diffraction spectra. No preferred orientation of the NCs is observed. A similar result has been obtained for the samples from the second group having small NCs. Values of $d = 1.5$ and 2 nm were obtained when employing Scherrer's equation, while the average NC diameter determined by HREM was about twice as great as the one calculated from the x-ray diffraction spectra. It may be noted that in nc-Si:H/a-SiN_x superlattices it has also been found [15] that the size of Si NCs is equal to the sublayer thickness.

It is known [16] that the full width at half maximum of x-ray diffraction peaks depends not only on the NC size but also on existing microstrains and deformations in the NC network. The observed discrepancy between the average size of CdSe NCs determined with x-ray diffraction and HREM studies may be related to the existence of a high level of microstrains in the nanocrystals, even after annealing the samples for 90 min at 673 K. In order to find some corroboration for this suggestion, the approximate levels of the microstrains were estimated

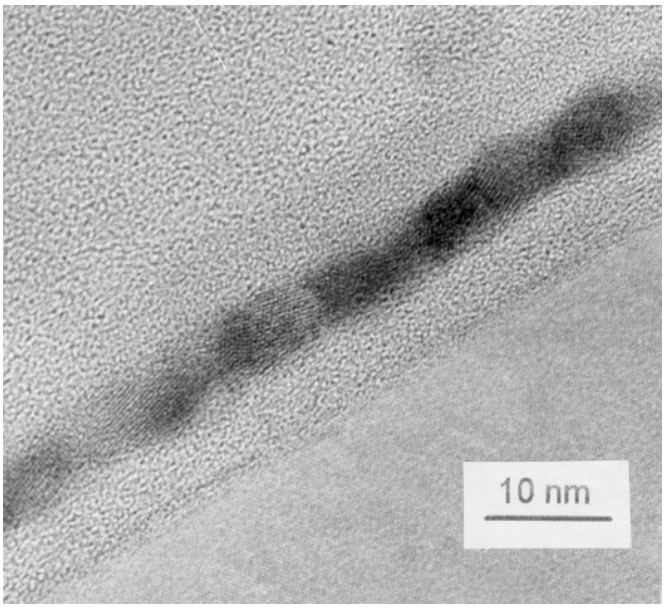

Figure 2. HREM cross-section of a SiO_x (5.8 nm)/CdSe (4.5 nm)/SiO_x (5.8 nm) structure. The micrograph shows the c-Si substrate in the lower right corner capped with a nanocrystalline CdSe layer sandwiched between two amorphous SiO_x layers. It is clear that the CdSe nanocrystallite size is equal to the CdSe layer thickness.

assuming the CdSe NC size and strain (ε) distributions to be Gaussian. The relation [16]

$$(\delta 2\theta \cos\theta/\lambda)^2 = 1/d^2 + 16\varepsilon^2(\sin\theta/\lambda)^2$$

was used, in which the respective average diameters were taken from the electron microscopy measurements. Values of around 20×10^{-3} and 28×10^{-3} have been obtained for nanocrystals having $d = 10.0$ and 5.0 nm respectively. They are close to the values of 20–22 $\times 10^{-3}$ calculated [17] for the CdSe layers of a free-standing CdS/CdSe superlattices with layers of equal thickness. A value of $\varepsilon \approx 49 \times 10^{-3}$ has been determined for NCs having $d = 3.0$ nm, which indicates that, as it might be expected, the level of microstrains rises with decreasing NC size. Therefore, we accept that the NC size in SiO_x/CdSe SLs is equal to the respective CdSe sublayer thickness. Throughout the subsequent part of the paper we use this thickness.

3.2. Urbach tail absorption

The CPM method is widely used ([12–14], and references therein) in order to study subband absorption of photoconductive thin films and superlattices. Energy dependences of the absorption coefficient, α (in arbitrary units), of SiO_x/CdSe SLs having CdSe sublayer thickness of 2.5, 3.5, 4.0, 5.0 and 10.0 nm are shown in figure 3. One can see a size-induced blue shift of the Urbach absorption tail as CdSe sublayer thickness decreases from 10 to 4.0 nm. This blue shift is followed by a red one for the SLs having $d_{CdSe} = 3.5$ and 2.5 nm. Our previous studies have shown [10] that, although CdSe sublayers of SiO_x/CdSe SLs are nanocrystalline, an overall three-dimensional carrier (and phonon) confinement does not exist and the carriers are confined only along the SL axis. In this case the optical band gap of the SLs is determined by electron transitions from the first mini-bands of the valence and conduction bands. The observed optical absorption tail is connected [13, 14] with absorption

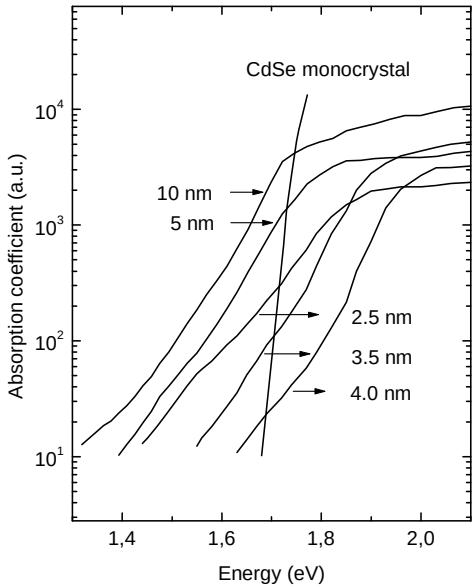

Figure 3. Band and Urbach tail absorption of SiO_x/CdSe SLs with various CdSe sublayer thicknesses (denoted by arrows to the respective curve). In all samples the Urbach absorption tail may be divided into two parts: (i) an exponential high-energy part and (ii) a low-energy part with a superimposed absorption. The last is attributed to electron transitions from surface defect states to the conduction band. Urbach absorption tail of CdSe monocrystals [17] is given for comparison.

in the localized tail states of the first mini-band of the valence band. It has been shown [18] that in disordered materials the rise of the level of disorder leads to both: (i) a reduction of the experimentally determined optical energy gap (at a constant mean energy gap) and (ii) a broadening of the optical absorption tail. Therefore, the observed unusual red shift in the SLs with $d_{CdSe} = 3.5$ and 2.5 nm may be related to a high level of disorder in the CdSe sublayers, caused by the high density of SiO_x–CdSe and CdSe–CdSe interfaces in these sublayers. It can also be seen from figure 3 that the high-energy part of the absorption tail is exponential and its slope is almost the same in the most SiO_x/CdSe SLs. Moreover, in all spectra a non-exponential part is well expressed in the low-energy region of the absorption tail. A more careful analysis of the absorption curves indicates that, in general, the thinner the CdSe sublayers, the shorter the exponential part of the tail absorption. Due to the low photoconductivity of the second group of samples, only a short exponential tail has been observed. It has been established that the tails of these samples are broader than those of all SLs. It may be assumed [18] that the level of disorder in the CdSe NCs in SiO_x matrix is higher than that in the CdSe sublayers of SiO_x/CdSe SLs. However, since the nature of the exponential absorption in NCs is unclear, the discussion bellow will concern only the results obtained on the SLs.

The subband absorption measured by photocurrent methods is usually related [12–14] to electron transitions: (i) from the neutral, exponentially distributed localized states of the valence band (vb) tail to the bottom of the conduction band (cb) and (ii) from other (neutral and/or charged) defect states, situated above the top of the vb, to the cb. As was mentioned above, the broader the Urbach tail, the higher the structural disorder in the sample [18]. The Urbach tail in our samples is significantly broader than that of CdSe monocrystals [19] (see figure 3), which indicates that the crystal network of CdSe NCs is much more disordered than that of monocrys-

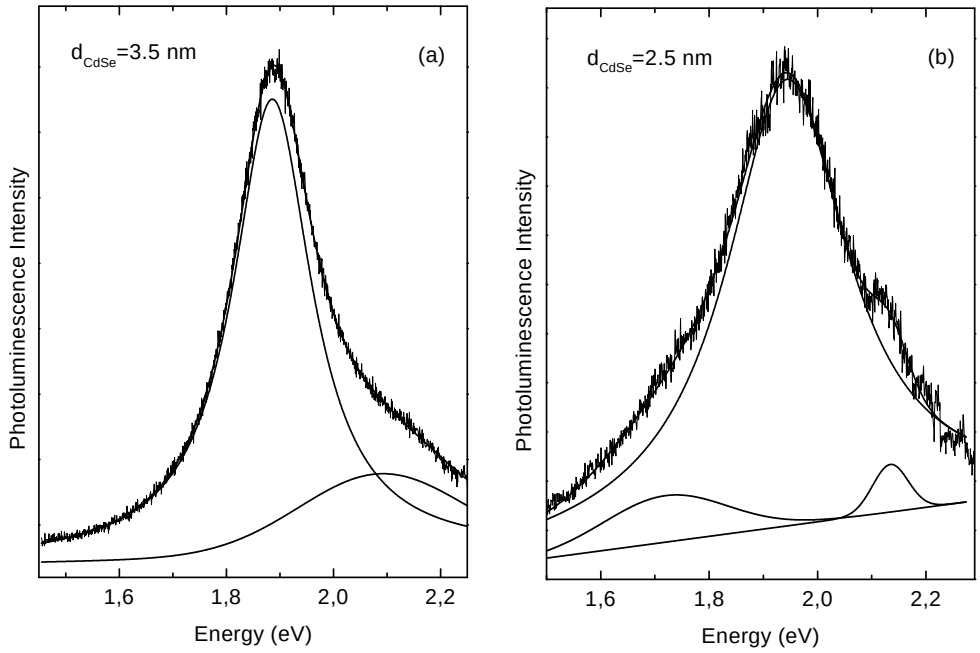

(a) (b)

Figure 4. Room-temperature photoluminescence spectra of SiO_x/CdSe SLs with CdSe sublayer thickness of 3.5 nm (a) and 2.5 nm (b) excited by the 530.9 nm Kr^+ laser line and fitted by two (a) or three (b) luminescence bands.

tals. This result supports the above given explanation of the observed great difference in the average NC size determined by means of x-ray diffraction and HREM. As for the observed non-exponential absorption, it may be related to superimposed absorption in some defect states whose levels are located in the region of the vb tail. From the absorption curves exhibited in figure 3, an energy of more than 0.3 eV (above the top of the first mini-band in the valence band of CdSe sublayers) may be roughly estimated for the position of such defect levels.

3.3. Room-temperature photoluminescence

Room-temperature photoluminescence spectra excited with the 530.9 nm Kr^+ laser line of two SiO_x/CdSe SLs having $d_{CdSe} = 3.5$ nm [10] and 2.5 nm are shown in figures 4(a) and 4(b) respectively. A detailed description of the set-up used for the photoluminescence measurements has been given in [10]. The spectra of SiO_x/CdSe SLs studied ($d_{CdSe} \geqslant 3.5$ nm) were well fitted to two bands displayed in figure 4(a). The strong low-energy Lorentzian band has been related [10] to radiative electron transitions from the bottom of the conduction to the top of the valence band of CdSe sublayers. The weak Gaussian band at about 2.1 eV may be assigned to recombination either in Si clusters formed in the SiO_x ($x \approx 1.5$) sublayers or in some very small isolated CdSe NCs. Only in the SL having the thinnest CdSe sublayers ($d_{CdSe} = 2.5$ nm) a third weak band is observed on the low-energy side of the Lorentzian band. It peaks at 1.78 eV and its full width at half maximum (FWHM) is $\sim$0.35 eV.

A great red shift (0.3–0.5 eV) with respect to the optical band gap and big FWHM value (0.2–0.5 eV) are characteristic for the interface defect state photoluminescence in CdSe NCs embedded in glass matrix [4, 5, 7]. Hence, the band peaked at 1.78 eV may be related to

radiative recombination through some interface defects (either at the SiO_x–CdSe interfaces or at the boundaries between CdSe NCs) in the CdSe sublayers of SiO_x/CdSe SLs. On the other hand, in the room-temperature photoluminescence spectra of CdSe NCs embedded in thin-film SiO_x matrix a strong wide photoluminescence band has been observed [20]. As its intensity was strongly dependent on the NC size, it was ascribed to recombination via defects at the SiO_x–CdSe interface. The energy position of this band (1.82–1.86 eV) is very close to the position of the 1.78 eV band observed in the SL spectrum. The last coincidence, together with the great FWHM of the 1.78 eV band, implies that in SiO_x/CdSe SLs this band may also be related to defect states at the SiO_x–CdSe interface of the CdSe NCs. Following Jungnickel and Henneberger [4], we assume that a radiative recombination of electrons from the conduction band with holes captured by deep acceptor-like defects takes place. Taking in mind that in SiO_x/CdSe SLs the optical band gap of CdSe sublayers having thickness of 2.5 nm is about 2.1 eV [10], one may estimate that these acceptor defects should be disposed at 0.32 eV above the top of the valence band. This value is a bit greater than that of 0.2 eV found in CdS_xSe_{1-x} doped glasses [21].

3.4. Thermally stimulated currents

The method of thermally stimulated currents was widely used [22] in order to investigate the position and concentration of traps in a great variety of crystalline as well as amorphous semiconductors. Thermally stimulated currents measured on three different samples: (i) CdSe single layer having microcrystalline-amorphous structure [23]; (ii) SiO_x/CdSe(2.5 nm) SL and (iii) thin SiO_x film doped with CdSe NCs having average size of 6 nm are shown in figure 5. Four well-expressed TSC maximums at about 190, 209, 253 and 285 K and two shoulders at $T \approx 225$ and 305 K are seen in the TSC curve of the single layer. In the TSC spectrum of the SL a relative current increase is displayed in the 220–250 K region. Finally, one can see that in the CdSe doped SiO_x film the TSC maximums at 190 and 209 K disappear, but two new maximums at about 220 and 240 K are well expressed as the latter is very strong and asymmetric to the high energies.

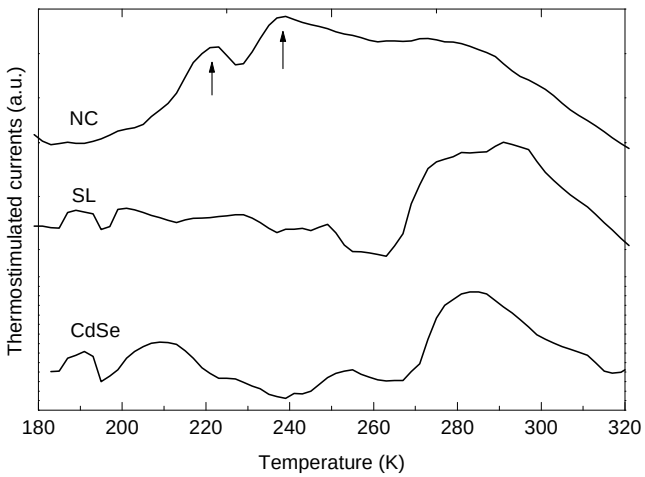

Figure 5. Thermally stimulated currents measured on a CdSe single layer having microcrystalline-amorphous structure, a SiO_x/CdSe (2.5 nm) SL and a thin SiO_x film doped with CdSe NCs with an average size of 6.0 nm. Two new TSC maximums at about 220 and 240 K (denoted by arrows) emerge in the low-dimensional samples. The magnitude of these maximums increases with increasing surface-to-volume ratio in CdSe NCs.

The positions of the TSC maximums observed in the CdSe single layer are in a general agreement with those reported by other authors [24, 25]. Our further discussion will be concentrated on the new maximums emerging in the TSC spectra of the samples having CdSe NCs. It is seen from figure 5 that the relative magnitude of thermally stimulated currents in the region 220–240 K is much higher in the composite SiO_x–CdSe film than in the SiO_x/CdSe SL. Bearing in mind that in the composite SiO_x–CdSe films the relative part of CdSe–CdSe interfaces should be marginal, one may assume that defects responsible for the observed new TSC maximums are created at the SiO_x–CdSe interface. In order to make a rough estimation of the energy position E_t of both traps we employed the relationship $E_t \approx 18\,kT$ [25], where k is the Boltzman constant. Values of 0.34 eV and 0.37 eV were obtained for the 220 K and 240 K maximum respectively. These values are close to that of 0.32 eV, determined from the photoluminescence measurements in SiO_x/CdSe SLs. As the concentration of both traps depends on surface-to-volume ratio in CdSe NCs, one can assume that, at least, one of these traps corresponds to the acceptor-like defects connected with the photoluminescence band at 1.78 eV and superimposed absorption discussed above. We speculate that this may be the strong band at 240 K as its asymmetry would explain the fact that the absorption superimposed on the low-energy part of the Urbach tail is extended in a wide-energy region. Indeed, the asymmetry of the TSC maximum to high temperatures should reflect a relatively wide distribution of defect states to the centre of the forbidden gap.

Thermally stimulated current ITSC in photoconductors may be generally described by the relation $I_{TSC} \sim e(n, p)\mu_{n,p}\tau_{n,p}$ where e is the electron charge, n, p is the concentration of electrons or holes thermally excited from an electron or hole trap to the cb or vb respectively and $\mu_{n,p}\tau_{n,p}$ is the drift mobility and life-time of electrons (sub 'n') or holes (sub 'p'). It is seen from figure 5 that the maximum at 240 K in the TSC spectrum of the composite SiO_x–CdSe film (related to acceptor defects) is stronger than the wide maximum between 270–300 K related to electron traps [25]. On the other hand, it is well known [19] that in CdSe the drift mobility of holes is more than one order of magnitude lower than that of electrons and that the lifetime of photogenerated holes is shorter than the one of electrons. Hence, a qualitative conclusion can be made that the great magnitude of the 240 K maximum should correspond to a quite high concentration of acceptor defect states at the SiO_x–CdSe interface.

In order to make a quantitative estimation of the concentration of the acceptor defects, we turn back to the fact that in the low-energy part of the Urbach tail the defect state absorption in the SLs exceeds that in the localized vb tail states. It may be assumed that the concentration of the surface defect states (N_t), at the starting point of the deviation from the high-energy exponential part of the Urbach tail, is of the same order as that of the tail states (N_u). The relationship $N_t \approx N_u \approx N_v \exp\{-(E - E_v)/E_u\}$, valid for distribution of the defect states in the valence band tail [26] may be used. Accepting $N_v \approx 10^{21}$ cm^{-3} [13] for the density of states at the top of the valence band E_v, $E_u = 0.055$ eV for the slope of the Urbach tail absorption and $(E - E_v) = 0.2$–0.3 eV (see figure 3), values around 10^{19} cm^{-3} were obtained for the concentration of the acceptor defect states. These values are much higher than the concentration of own defects in crystalline CdSe [27]. They are close to defect concentrations found in disordered amorphous materials [26].

4. Conclusions

As mentioned above, the available information on the energy position and photoinduced changes of interface defect states responsible for the high optical nonlinearity observed in $CdS_{1-x}Se_x$ doped glasses [5] is quite insufficient. On the other hand, it is well known that the electrical and photoelectrical properties of semiconductors are more sensitive to defects

and impurities than their optical properties. For this reason, in an attempt to obtain some information about defect states at the SiO_x–CdSe interface, parallel electrical, photoelectrical and photoluminescence measurements have been carried out on CdSe nanocrystals embedded in thin film SiO_x matrix and such forming two-dimensional nanocrystalline CdSe sublayers of SiO_x/CdSe superlattices. The constant photocurrent measurements of the Urbach tail absorption of SiO_x/CdSe SLs have shown that electron transitions from some acceptor defect states to the conduction band of CdSe sublayers are responsible for the absorption superimposed on the Urbach tail. It has also been estimated that their concentration attains values of about 10^{19} cm^{-3}. Furthermore, a gradual increase of two new maximums in thermally stimulated currents has been observed with increasing surface-to-volume ratio of CdSe nanocrystals. It has been assumed that the maximum at 240 K ($E_t \approx 0.37$ eV) is due to acceptor defects at the SiO_x–CdSe interface. Finally, the position and great FWHM of the photoluminescence band observed in the SL having the thinnest CdSe sublayers and in CdSe NC doped SiO_x thin films have been considered as additional proofs for the existence of acceptor defect states through which radiative recombination takes place.

Acknowledgments

This work was supported by the National Scientific Foundation of the Bulgarian Ministry of Education and Science under Contract F-505.

References

[1] Roussignol P, Ricard D, Lukasik J and Flytzanis C 1987 *J. Opt. Soc. Am.* **4** 5–13
[2] Saltiel S M, van Wonterghem B and Rentzepis P M 1990 *Opt. Commun.* **77** 59–62
[3] Kang K, Kepner A D, Hu Y Z, Koch S W, Payghambrian N, Li C Y, Takada T, Kao Y and Mackenzie J D 1994 *Appl. Phys. Lett.* **64** 1487–90
[4] Jungnickel V and Henneberger F 1996 *J. Lumin.* **70** 238–52
[5] Flytzanis C, Ricard D and Schanne-Klein M C 1996 *J. Lumin.* **70** 212–21
[6] Bawendi M G, Wilson W L, Rotberg L, Carroll P J, Jedju T M, Steigerwall M L and Brus L E 1993 *Phys. Rev. Lett.* **65** 1623–6
[7] Arai T and Matsuishi K, 1996 *J. Lumin.* **70** 281–93
[8] Nesheva D and Levi Z 1997 *Semicond. Sci. Technol.* **12** 1319–22
[9] Ionov R and Nesheva D 1992 *Thin Solid Films* **213** 230–4
[10] Nesheva D, Raptis C and Levi Z 1998 *Phys. Rev.* B **58** 7913–20
[11] Popescu M, Sava F, Lorinczi A, Vateva E, Nesheva D, Tschaushev G, Mihailescu I N, Koch P-J, Obst S and Bradaczeck H 1998 *Proc. SPIE* **3405** 964–8
[12] Marshall J M, Pickin W, Hepburn A R, Main C and Bruggemann R 1991 *J. Non-Cryst. Solids* **137/138** 343–6
[13] Wang F, Fischer T, Muschik T and Schwarz R 1993 *Phil. Mag.* B **68** 737–51
[14] Nesheva D, Arsova D and Levi Z 1994 *Phil. Mag.* B **70** 205–13
[15] Huang X, Wu Zh Li W, Chen K, Chen X and Liu Z 1996 *J. Non-Cryst. Solids* **198–200** 821–4
[16] Sen S, Halder S K and Gupta S P S 1975 *J. Phys. Soc. Japan* **38** 1641–7
[17] Gusso M, De Caro L and Tapfer L 1997 *Solid State Commun.* **101** 665–9
[18] O' Leary S K, Zukotynski S and Perz J M 1997 *J. Non-Cryst. Solids* **210** 249–53
[19] Landolt-Bornstein 1982 *Numerical Data and Functional Relationships in Science and Technology, New Series* vol 17, subvolume b, ed K-H Hellewege (Berlin: Springer) p 217
[20] Nesheva D, Raptis C, Levi Z, Popovic Z and Hinic I 1999 *J. Lumin.* at press
[21] Zhang X and Hamaguchi H 1997 *Z. Phys.* D **40** 44–7
[22] Milnes A G 1973 *Deep Impurities in Semiconductors* (New York: Wiley) ch 9
[23] Nesheva D, Arsova D and Ionov R 1993 *J. Mater. Sci.* **28** 2183–6
[24] Kindleysides L and Woods J 1970 *J. Phys. D: Appl. Phys.* **3** 451–61
[25] Okimura H and Sakai Y 1968 *Japan. J. Appl. Phys.* **7** 731–8
[26] Mott N F and Davis E A 1979 *Electron Processes in Non-Crystalline Materials* (Oxford: Clarendon) ch 6
[27] Robinson A L and Bube R H 1971 *J. Appl. Phys.* **43** 5280–95